

## Conditional deletion of Cadherin 13 perturbs Golgi cells and disrupts social and cognitive behaviors


M. Tantra, L. Guo, J. Kim, N. Zainolabidin, Volker Eulenburg, G. J. Augustine, A. I. Chen

### Angaben zur Veröffentlichung / Publication details:

Tantra, M., L. Guo, J. Kim, N. Zainolabidin, Volker Eulenburg, G. J. Augustine, and A. I. Chen. 2018. "Conditional deletion of Cadherin 13 perturbs Golgi cells and disrupts social and cognitive behaviors." *Genes, Brain and Behavior* 17 (6): e12466.  
<https://doi.org/10.1111/gbb.12466>.

## ORIGINAL ARTICLE

# Conditional deletion of Cadherin 13 perturbs Golgi cells and disrupts social and cognitive behaviors

M. Tantra<sup>1,2</sup> | L. Guo<sup>1,2</sup> | J. Kim<sup>3</sup> | N. Zainolabidin<sup>1,2</sup> | V. Eulenburg<sup>5</sup> | G. J. Augustine<sup>3,4</sup> | A. I. Chen<sup>1,2,4</sup> 

<sup>1</sup>School of Biological Sciences, Nanyang Technological University (NTU), Singapore

<sup>2</sup>School of Life Sciences, University of Warwick, Coventry, UK

<sup>3</sup>Lee Kong Chian School of Medicine, Nanyang Technological University (NTU), Singapore

<sup>4</sup>Institute of Molecular and Cell Biology, Singapore

<sup>5</sup>Institute of Biochemistry, Friedrich-Alexander University Erlangen-Nuremberg, Erlangen, Germany

## Correspondence

A. I. Chen, 11 Mandalay Road, Clinical Sciences Building Level 12, Singapore 308232.

Email: albert.chen@ntu.edu.sg

## Funding information

National Medical Research Council, Grant/Award number: NMRC/CBRG/0075/2014; Singapore Ministry of Education, Grant/Award number: RG124/15

Inhibitory interneurons mediate the gating of synaptic transmission and modulate the activities of neural circuits. Disruption of the function of inhibitory networks in the forebrain is linked to impairment of social and cognitive behaviors, but the involvement of inhibitory interneurons in the cerebellum has not been assessed. We found that *Cadherin 13* (*Cdh13*), a gene implicated in autism spectrum disorder and attention-deficit hyperactivity disorder, is specifically expressed in Golgi cells within the cerebellar cortex. To assess the function of *Cdh13* and utilize the manipulation of *Cdh13* expression in Golgi cells as an entry point to examine cerebellar-mediated function, we generated mice carrying *Cdh13-floxed* alleles and conditionally deleted *Cdh13* with *GlyT2::Cre* mice. Loss of *Cdh13* results in a decrease in the expression/localization of GAD67 and reduces spontaneous inhibitory postsynaptic current (IPSC) in cerebellar Golgi cells without disrupting spontaneous excitatory postsynaptic current (EPSC). At the behavioral level, loss of *Cdh13* in the cerebellum, piriform cortex and endopiriform claustrum have no impact on gross motor coordination or general locomotor behaviors, but leads to deficits in cognitive and social abilities. Mice lacking *Cdh13* exhibit reduced cognitive flexibility and loss of preference for contact region concomitant with increased reciprocal social interactions. Together, our findings show that *Cdh13* is critical for inhibitory function of Golgi cells, and that *GlyT2::Cre*-mediated deletion of *Cdh13* in non-executive centers of the brain, such as the cerebellum, may contribute to cognitive and social behavioral deficits linked to neurological disorders.

## KEYWORDS

autism spectrum disorder, Cadherin 13, cerebellum, cognitive flexibility, GABAergic interneurons, GlyT2, Golgi cells, reciprocal social interaction

## 1 | INTRODUCTION

The cerebellum controls motor coordination, fine motor movement and motor learning, but there is increasing evidence supporting its contribution to cognitive and motivational processes.<sup>1,2</sup> Dysfunction of the cerebellum has been associated not only with motor conditions but also with disorders such as autism spectrum disorder (ASD), attention-deficit hyperactivity disorder (ADHD) and fragile-X

syndrome.<sup>3-6</sup> Despite the emerging support for a link between cerebellum and neurological disorders, little is known about how disruptions within the cerebellar network contribute to phenotypes ranging from motor to higher brain function such as cognitive processing and social behaviors. Moreover, studies linking cerebellar dysfunction and neurodevelopmental disorders have focused primarily on Purkinje cells.<sup>5,7-9</sup>

Golgi cells are dual GABAergic and glycinergic interneurons in the cerebellar cortex that have been proposed to contribute to the reduction and filtering of mossy fiber input to granule cells before

Martesa Tantra and Lanboling Guo contributed equally to this study.

This is an open access article under the terms of the Creative Commons Attribution-NonCommercial-NoDerivs License, which permits use and distribution in any medium, provided the original work is properly cited, the use is non-commercial and no modifications or adaptations are made.

© 2018 The Authors. Genes, Brain and Behavior published by International Behavioural and Neural Genetics Society and John Wiley & Sons Ltd.

they innervate Purkinje cells.<sup>11,10–12</sup> Golgi cell-mediated neural circuits thus play an important role in sensory-motor integration.<sup>13</sup> Ablation of Golgi cells in mice results in severe ataxia followed by subsequent mild motor coordination deficits.<sup>14</sup> Golgi cells play critical roles in oculomotor performance by regulating distinct subtypes of eye movements.<sup>15,16</sup> In addition, computational studies have suggested that Golgi cells generate behaviorally relevant patterns of activity.<sup>17,18</sup> Despite the importance of Golgi cells in sensory motor processing and motor adaptation, the molecular mechanisms underlying their synaptic functions are not well understood. Moreover, whether disruption in Golgi cell activity contributes to deficits in nonmotor behaviors has not been assessed in detail.

Many members of the cadherin superfamily are expressed in the nervous system with distinct spatial and temporal expression patterns, and have been linked to neurological disorders.<sup>19–23</sup> In particular, *Cdh13* has been shown to regulate many neuronal processes. Both excitatory and inhibitory synaptic function in the hippocampus depends on *Cdh13* expression,<sup>24,25</sup> and the complete deletion of *Cdh13* results in impaired spatial learning and conditioned place preference.<sup>25,26</sup> In addition to synapse formation, *Cdh13* controls neuronal migration and specificity of axonal targeting in the developing cerebral cortex and spinal cord.<sup>27–29</sup> While evidence for the role of *Cdh13* in the nervous system is growing,<sup>25,27,29–32</sup> its expression and functional relevance in the cerebellum have not yet been examined.

Human genetics studies have implicated *CDH13* mutations with altered social behaviors in ASD patients.<sup>33</sup> In addition, genome-wide association studies have linked *CDH13* with violent behavior.<sup>34</sup> However, analysis of the role of *Cdh13* in mice to date has relied on deletion of *Cdh13* in all tissues, so the critical regions that require *Cdh13* to mediate motor and cognitive behaviors have not been defined. Here, we report the selective expression of *Cdh13* in Golgi cells of the mouse cerebellum. To examine the link between *Cdh13* and the organization and function of cerebellar inhibitory circuits, we generate mice carrying *Cdh13-floxed* alleles and delete *Cdh13* in Golgi cells and restricted regions outside the cerebellum. We assess consequences of conditional *Cdh13* deletion on the synaptic constituents and electrophysiological properties of Golgi cells as well as motor and cognitive behaviors.

## 2 | MATERIALS AND METHODS

### 2.1 | Mouse strains

The following mice were used in this study: *GlyT2::Cre* (line 122.2),<sup>35</sup> *Rosa::lox-stop-lox-eYFP* (The Jackson Laboratory),<sup>36</sup> and *Cdh13<sup>fl/fl</sup>* mice were generated with embryonic stem (ES) cells containing the *Cdh13* allele with *loxP* sites flanking exon 3 from the European Mouse Mutant Cell Repository (Jm8A3.N1). *GlyT2::Cre; Cdh13<sup>fl/fl</sup>* (*GlyT2-Cdh13<sup>-/-</sup>*) mice were generated by crossing male *GlyT2::Cre; Cdh13<sup>fl/+</sup>* or *GlyT2::Cre; Cdh13<sup>fl/fl</sup>* with female *Cdh13<sup>fl/fl</sup>* mice. For collection of tissue at different embryonic and postnatal stages, breeders were housed together between 8 and 12 hours at night, and the male and female breeder mice were then separated and vaginal plugs were examined. We designated noon of the following day as E0.5.

The histology of tissues obtained at different time points were carefully cross-referenced with images in the Prenatal Mouse Brain Atlas,<sup>37</sup> and Developing Mouse Brain (Allen Brain Atlas). All experiments conducted were approved by the local BRC Institutional Animal Care and Use Committee.

### 2.2 | Southern blotting

Primers used to generate 5' DNA probe: forward 5' ATTGC TATTGCGTGGCTGTGTGAGG 3'; reverse 5' TGAGAGCCCTGGTCTCTTGTGAGC 3'. 3' DNA probe: forward 5' TGGAAGTCTTGACTCA AGTAGAGATG 3'; reverse 5' ACCAACTCCGGCCTATCTACTTC 3'. The probe was labeled with PCR DIG probe synthesis kit (Roche, #11636090910, Hoffman-La Roche, Basel, Switzerland). Genomic DNA was isolated with phenol-chloroform, and digested by using *EcoRI* or *StuI*, plotted on a 0.8% agarose gel and transferred to a Hybond-N+ membrane (Amersham Biosciences, RPN225B, Amersham Biosciences, Little Chalfont, UK). Hybridization was performed at 60°C with ExpressHyb Hybridization Solution (Clontech Laboratories, #636831). After hybridization, the membrane was washed and blocked with DIG wash and block buffer set (Roche, #11585762001) and incubated with antibody (Anti-Digoxigenin-AP Fab fragments, Hoffman-La Roche, Basel, Switzerland, #11093274910) for 40 minutes to 1 hour. The membrane was incubated with CSPD (Roche, #11755633001) before exposure.

### 2.3 | In situ hybridization

Chromogenic and fluorescent *in situ* hybridization were performed according to previously published work.<sup>38–40</sup> The RNA probe was designed to target the sequence between the second and the third exon of mouse *Cdh13* mRNA. The primers used to make the probe were: forward 5' CAACGAGAAGCTGCACTACG 3' and reverse 5' GCGCTAATACGACTCACTATAGGGGGACACCACAATGGACCTCT 3'. Mouse brains were sectioned into 18 µm and 60°C was used as incubation temperature for hybridization. For fluorescent *in situ* hybridization, TSA plus cyanine 5 System (PerkinElmer, NEL745001KT PerkinElmer, Waltham, MA, USA) and TSA plus fluorescein System (PerkinElmer, NEL741001KT) were used for signal amplification. In addition, *in situ* hybridization analysis performed on tissues after viral transduction utilized hybridization solution containing urea utilized hybridization solution containing urea and 50°C was used for hybridization.

### 2.4 | Immunohistochemistry

#### 2.4.1 | Staining of slice-mounted sections

Cryosections sliced into 18 µm were mounted on glass slides, washed with 0.2% Triton-X and blocked in blocking buffer (phosphate-buffered saline [PBS], 0.1% Triton-X [OmniPur], 2% horse serum [Invitrogen]). Primary antibody was diluted into blocking buffer and incubated overnight at 4°C. Then, washing buffer (PBS, 0.1% Triton-X [OmniPur]) was used to wash slices for 3 times and slices were incubated with secondary antibody. Next, slices were washed again with washing buffer and mounted slides with coverslip and mounting

reagent (ProLong Gold antifade reagent [Life Technologies, Carlsbad, CA, USA]).

Primary antibodies used in the immunohistochemical staining: mouse anti-GAD67 (1:500, Merck, MAB5406); rat anti-GFP (1:1000, Nacalai Tesque, GF090R), mouse anti-mGluR2 (1:1500, Advanced Targeting System, AB-N32), rabbit anti-Neurogranin (1:1000, Merck, AB5620). Goat anti-Olig2 (1:250, R&D), mouse anti-Calbindin (1:5000, Swant).

## 2.4.2 | Image analysis

All images were collected on a confocal microscope (LSM710; Zeiss, Oberkochen, Germany). Image acquisition parameters were kept the same between control and experimental groups for each experiment. Quantification of images was performed using NIH ImageJ (NIH, Bethesda, MD, USA version 1.46r). The protein expression was calculated by measuring the maximal brightness of the 6 brightest layers of the image stack in  $53 \mu\text{m} \times 53 \mu\text{m}$  regions from Crus 2 and lobule IX of both control and *GlyT2-Cdh13*<sup>-/-</sup> mice.

## 2.5 | In vitro electrophysiology

Mice aged between 26 and 35 days were sacrificed under deep anesthesia and the cerebellum was quickly isolated. Sagittal cerebellar sections (250  $\mu\text{m}$ ) were cut at the room temperature and incubated at 34°C for 1 hour in the oxygenated standard extracellular solution containing (in mM) 126 NaCl, 24 NaHCO<sub>3</sub>, 1 NaH<sub>2</sub>PO<sub>4</sub>, 2.5 KCl, 2.5 CaCl<sub>2</sub>, 2 MgCl<sub>2</sub>, 10 glucose, 0.4 ascorbic acid (pH 7.4/95% O<sub>2</sub>/5% CO<sub>2</sub>). Whole-cell patch clamp recordings were conducted at room temperature as previously described.<sup>41</sup> For whole-cell recordings from Golgi cells, electrodes (4–7 M $\Omega$ ) were filled with a CsCl-based internal solution containing (in mM): 140 CsCl, 4 NaCl, 0.5 CaCl<sub>2</sub>, 10 HEPES (4-(2-hydroxyethyl)-1-piperazineethanesulfonic acid), 5 EGTA (egtzacic acid), 2 MgATP (Manganese adenosine triphosphate), 0.4 Guanosine triphosphate trisodium salt (Na3GTP) (pH 7.3, ~290 mOsm). Both inhibitory postsynaptic currents (IPSCs) and excitatory postsynaptic currents (EPSCs) were recorded under voltage clamp with a holding potential of -60 mV and the access resistance was compensated. Neurobiotin (0.5%; Vectorlabs, Burlingame, California) was added in the internal solution to identify Golgi cell morphology.

Spontaneous IPSCs were measured after blocking excitatory synaptic inputs by addition of glutamate receptor antagonists, NBQX (10  $\mu\text{M}$ ) and D-AP5 (50  $\mu\text{M}$ ). Spontaneous EPSCs were measured during application of SR95531 (10  $\mu\text{M}$ ) and strychnine (0.3  $\mu\text{M}$ ) to block GABAergic and glycinergic inputs. After recording spontaneous IPSCs or EPSCs, tetrodotoxin (TTX; 1  $\mu\text{M}$ ) was further added in bath solution to record miniature IPSCs or EPSCs. The frequency and amplitude of spontaneous and miniature IPSCs/EPSCs were analyzed in 5-minute periods after a period of drug equilibration (5–10 minutes).

## 2.6 | Behavioral analyses

After weaning and during the period of behavioral testing, male mice were group-housed in standard plastic cages and kept under

temperature-controlled environment ( $21 \pm 2^\circ\text{C}$ ) on 12 hours light/dark cycle with food and water ad libitum, unless stated otherwise. For behavioral analysis, only male *GlyT2-Cdh13*<sup>-/-</sup> mutant mice and *Cdh13*<sup>fl/fl</sup> control mice were used. To minimize behavioral variability that might occur due to hormonal changes related to the estrous cycle, we did not analyze female mice.<sup>42,43</sup> *GlyT2-Cdh13*<sup>-/-</sup> mice were generated by breeding *Cdh13*<sup>fl/fl</sup> females with *GlyT2-Cdh13*<sup>+/-</sup> or *GlyT2-Cdh13*<sup>-/-</sup> males. All experiments were conducted by investigators unaware of the genotype, during the light phase of the day (between 8 AM and 6 PM). Adult male mice were run through a battery of tests covering basic behavioral, sensory, motor, cognitive and social functions, with the order of tests was oriented toward increasing invasiveness.

### 2.6.1 | Open field

Spontaneous activity in open field was tested in a gray Perspex arena (Biosystems Corporation, Singapore) (60  $\times$  60  $\times$  40 cm). The mouse was positioned in the center and allowed to explore the open field for 7 minutes. The behavior was recorded by a PC-linked overhead video camera. "Ethovision XT" software (Noldus, Wageningen, Netherlands) was used to calculate velocity and distance traveled which reflected the spontaneous activity and stay duration in the corner vs center and number of visits as read outs for novelty-induced anxiety of the mouse during the open field session.

### 2.6.2 | Rota-rod

Rota-rod is a test for motor function, balance and coordination and comprises a rotating drum (TSE GmbH, Bad Homburg, Germany) which was accelerated from 4 to 40 rotations per minute (rpm) over the course of 5 minutes. Each mouse was placed individually on a drum and the latency of falling from the drum was recorded using a stopwatch. To assess motor learning, the rota-rod test was repeated 24 hours later. Each mouse performed 6 trials in total.

### 2.6.3 | Odor habituation/dishabituation test

This test consists of sequentially presenting different odors and assessing the response of mice to each odor.<sup>44</sup> The sequence used was as followed: water, a nonsocial odor (rose) and 2 social odors (bedding swab from group-housed mice of the same sex). For nonsocial odor, the cotton tip was dipped in a solution containing food-grade rose artificial flavor (1:100 dilution, Star Brand, Malaysia). Social odor stimuli were prepared by swiping the cage bottom with a cotton tip. Each odor was presented in 3 consecutive trials for a duration of 2 minutes, with a 1-minute intertrial interval between presentation. The trial started when the cotton tip applicator containing the odor was presented into the cage lid. Time spent on sniffing the tip was recorded using a stopwatch.

### 2.6.4 | Marble burying

This test was used to assess digging behavior in mice. Mice were tested in plastic cages (34.5  $\times$  56.5  $\times$  18 cm) filled with 5 cm deep wood-chip bedding. On top of the bedding, 24 glass marbles were placed. The marbles were arranged in 6 rows with 4 marbles per row at a distance of 4 cm. Each mouse was placed into the cage and could

freely manipulate the marbles for 30 minutes. Number of buried marbles (to two-thirds their depth) was scored.

### 2.6.5 | Resident-intruder test

This test was used to study intermale aggression in adult male mice. As standard opponents (intruders), group-housed males of C57BL6/JInV background were used (InVivos, Singapore). An intruder was introduced into the home cage of the single-housed test resident. Observation started when the resident first sniffed the opponent and stopped at first attack (defined as bite) to prevent wounding, but lasted for 600 seconds if no attack occurred.

### 2.6.6 | Two-choice digging task

This task was performed as described previously.<sup>45–47</sup> This task relies on the digging behavior of mice and uses multimodal stimuli, though only one dimension of a stimulus (the texture of the bowl) predicts the location of the reward, while the other dimension (the texture of the bedding) provides irrelevant information and thereby serves as a distraction.

Adult male mice were trained in the task comprising a habituation, shaping and discrimination learning in a modified perspex box (30 × 18 × 12 cm) divided into 3 zones with removable dividers. Two digging bowls separated by a plastic panel were placed into each quarter section. Mice were food-deprived during the whole period of testing and habituated with testing apparatus and food reward (Honey Stars, Nestle). After 2 days of habituation and through the experiment, mice were maintained at 85% of free-feeding weight with water ad libitum. The shaping phase lasted for 2 days where mice were trained to dig in unscented bedding for food reward. Afterwards, mice were trained to perform a series of discrimination tasks: selecting a bowl dependent upon a stimulus in a particular dimension, either texture of the bedding or of the outer bowl. A correct choice led to a reward buried within the bowl, while an incorrect choice caused the trial to be terminated and access to the other bowl was denied.

Each trial was initiated by raising the divider allowing access to the 2 digging bowls, one of which was baited with reward. The first task presented was a series of simple discrimination: 2 stimuli were presented in one dimension (the outer bowl texture, aluminum foil vs paper wrap, commercially available) while the digging medium was similar in both bowls. Mice were trained to learn that one dimension, the outer bowl texture, is the target stimulus (contains food reward) and the other is irrelevant. Following the simple discrimination, a compound discrimination task was then applied: a second dimension (bedding—paper vs woodchip bedding—were introduced but still irrelevant, as the mouse was still required to discriminate between the 2 original stimuli (outer texture of the bowls). Next, mice were trained in an intradimensional (ID) shift: novel stimuli were introduced for both dimensions (new bedding and new bowl texture), the target dimension remained the same (outer bowl texture). After the compound discrimination and intradimensional set shift, a reversal phase of each was introduced, wherein the previously irrelevant stimuli became relevant and rewarded. We introduced an overtraining paradigm before proceeding to the second set of ID shift and its reversal.

During the overtraining phase, mice received the same pair of stimuli as in the reversal phase of the first ID for additional 60 trials. Discrimination learning involves both perceptual- and response-learning processes where mice were trained to pay attention to the relevant (rewarded) stimulus dimension,<sup>47</sup> and consequently mice produced bias responses toward the correct cue along the dimension. Overtraining has been shown to either facilitate or retard the subsequent phases of learning.<sup>48</sup> Therefore, we introduced overtraining as an additional challenge during discrimination learning to investigate the extent that *Cdh13* deletion influences discrimination learning. Following the overtraining, a second set of ID shift and its reversal were introduced with a new pair of stimuli. Throughout the sessions, trials to criterion and errors were recorded for each stage. Error was defined as digging into the bowl that was never baited. The mouse was considered to have reached criterion for each stage when it completed 8 correct choices within 10 trials.

### 2.6.7 | Reciprocal social interaction

This test was conducted as described previously.<sup>49</sup> The social interaction test was performed pairwise in a neutral arena (gray Plexiglas box, 30 × 30 × 30 cm). Pairs of unfamiliar mice of the same genotype were placed into the neutral arena for 10 minutes. The behavior of mice was recorded and scored by a trained observer who was “blinded” to the genotype of the mice. The time spent in social interaction (defined as staying in close contact) and numbers of contacts were registered. Also, contact was categorized and analyzed into nose-to-nose, nose-to-body and nose-to-anogenital area. The first 3 minutes of the interaction was analyzed separately to investigate whether social behavior in the novel and neutral arena was influenced by the novelty factor of the environment. Pairs of the same genotype were used to exclude potential confounding factors such as interactions induced by a wild-type control mouse in case of using a mutant-control pair.

### 2.6.8 | Gait analysis

The methods for analysis of gait pattern have been previously described.<sup>50,51</sup> In brief, the footprints were detected optically with a walkway designed based on disrupted total internal reflection.<sup>51</sup> First, mice were habituated to the walkway. After habituation, mice were permitted to walk freely within the walkway. The paw prints made were recorded using a high frame rate camera at 450 frames per second (fps) and the footprint patterns were analyzed by using PhotoShop CS6 to measure the length of each stride.

### 2.6.9 | Statistical analysis

All experimental data acquisition was performed by experimenters unaware of group assignment. Data presented were analyzed by Mann-Whitney *U* test to for genotype comparisons and/or analysis of variance (ANOVA) including post hoc testing for genotype and trials effects and interaction effects of genotype and experimental setup using GraphPad Prism version 6&7 (GraphPad Software, La Jolla, California).

### 3 | RESULTS

#### 3.1 | Specificity of the expression pattern and conditional deletion of *Cdh13* in the cerebellum

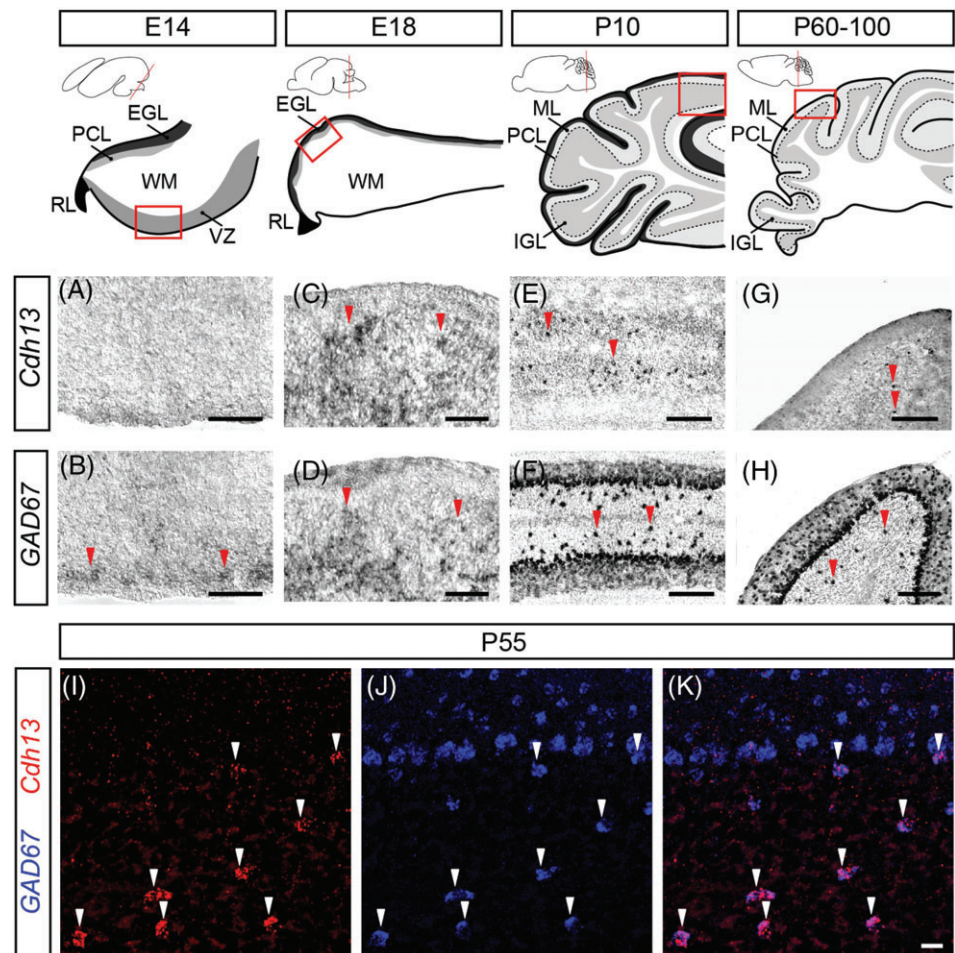
*Cdh13* is expressed in excitatory and inhibitory neurons in the developing mouse forebrain, spinal cord and dorsal root ganglion,<sup>28,29,52</sup> but details of *Cdh13* expression pattern in the cerebellum are not clear. To define the expression pattern of *Cdh13* in the cerebellum and determine whether *Cdh13* is expressed in excitatory and/or inhibitory neurons, we analyzed and compared the RNA expression of *Cdh13* in the developing and mature cerebellum with *GAD67*, a molecular marker for GABAergic inhibitory neurons.<sup>53</sup> During embryonic development, we observed limited *Cdh13* expression at E14 in the cerebellar ventricular zone where many *GAD67*<sup>+</sup> GABAergic precursors reside, consisting of mostly Purkinje and Golgi cell precursors (Figure 1A,B).<sup>54</sup> The expression of *Cdh13* becomes more prominent in the white matter layer of the cerebellum and coincides with *GAD67* expression at E18, and *Cdh13*<sup>+</sup> cells make up a subset of *GAD67*<sup>+</sup> cells at this stage (Figure 1C,D; Figure S1A-E). In the postnatal cerebellum, at P10 and P60, *Cdh13*<sup>+</sup> cells are found only in the internal granular layer (IGL) where *GAD67*<sup>+</sup> interneurons are located, but not in the Purkinje cell or molecular layer (Figure 1E-H). Colocalized *Cdh13* and *GAD67* expression confirms that *Cdh13* is expressed by GABAergic interneurons, including Golgi cells, located in the IGL of the cerebellum (Figure 1I-K). Our expression analysis, however,

does not exclude the possibility that Purkinje and stellate/basket cells transiently express *Cdh13* during embryonic and early postnatal stages.

In order to assess the functional relevance of *Cdh13* in the cerebellum, we set out to delete *Cdh13* in Golgi cells. We acquired ES cells from the European Mouse Mutant Cell Repository and generated mice carrying the *Cdh13* allele with *loxP* sites flanking exon 3 (*Cdh13*<sup>fl/fl</sup>) (Figure 2A). We confirmed the occurrence of homologous recombination of the targeting construct into the genome as well as the distinction in size of the floxed allele compared to the wild-type allele (Figure 2B,C). To delete *Cdh13* in cerebellar Golgi cells, we utilized a bacterial artificial chromosome (BAC) transgenic mouse line which specifically expresses Cre recombinase under control of the promoter for the *glycine transporter 2* gene (*GlyT2::Cre*).<sup>35</sup>

We first assessed the recombination ability of *GlyT2::Cre* mice by crossing them to *Rosa26::lox-stop-lox-YFP* mice and found recombined neurons sparsely located in the cortex, and no recombined neurons in the hippocampus.<sup>35</sup> In the cerebellum, YFP<sup>+</sup> neurons coexpress mGluR2 and Neurogranin, key molecular markers of cerebellar Golgi cells, indicating that *GlyT2::Cre* mice possess the ability to recombine in Golgi cells (Figure 2D-F).<sup>55</sup> In addition, we observed YFP<sup>+</sup> neurons in the deep cerebellar nuclei, consistent with previous reports<sup>56</sup> (Figure S2A-D,K-L). We note that *GlyT2::Cre* mice also mediates recombination in some Purkinje and stellate/basket cells consistent with previously described (Figure 2D).<sup>35</sup> The *GlyT2::Cre*-mediated recombination occurs during embryonic stages, and can be

**FIGURE 1** *Cdh13* is expressed by a subpopulation of GABAergic interneurons in the cerebellar cortex. A-H, Expression of *Cdh13* mRNA at embryonic and postnatal stages of development. At E14, *Cdh13* is not detected in the VZ (A), where limited *GAD67* expression is present (red arrows; B). At E18, the expression of *Cdh13* and *GAD67* is present in the WM layer of the cerebellum (red arrows; C, D). At postnatal stages P10-100, *Cdh13* and *GAD67* are both found in the IGL of the cerebellar cortex (red arrows; E-H). EGL, external granular layer; PCL, Purkinje cell layer; RL, rhombic lip; WM, white matter; VZ, ventricular zone; ML, molecular layer; IGL, internal granular layer. I-K, Double fluorescent *in situ* hybridization shows that *Cdh13* and *GAD67* mRNA are colocalized in the IGL (white arrows; I-K). *GAD67* signal is detected in inhibitory neurons in all 3 layers (J), but *Cdh13* signal is only detected in the IGL (white arrows; I, K). Scale bar = 200  $\mu$ m (A-H), 20  $\mu$ m (I-K)



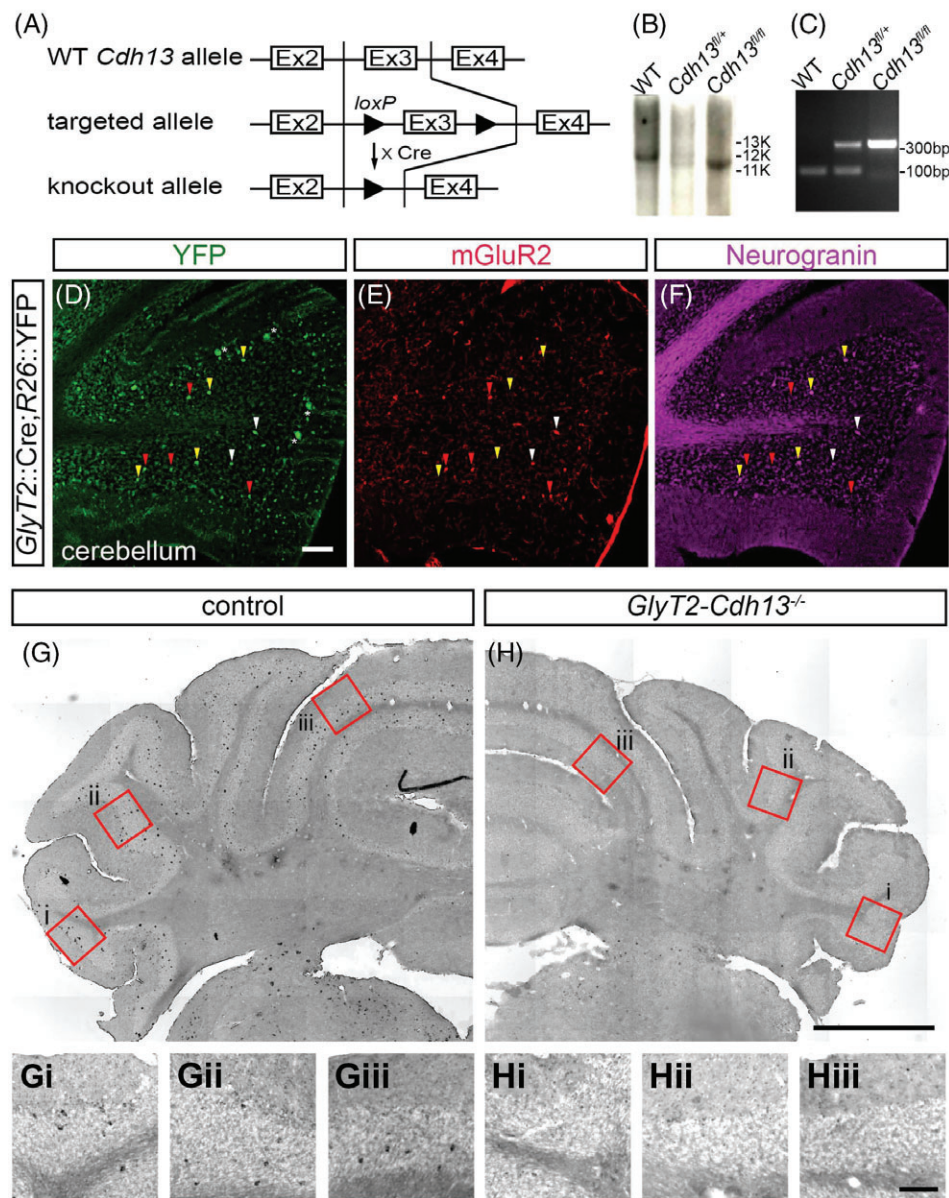


**FIGURE 2** *GlyT2::Cre* mediates *Cdh13* deletion in cerebellar Golgi cells. A, Strategy for generation of *Cdh13* conditional knockout mice. Exon 3 flanked by *loxP* is removed by Cre expression in *GlyT2::Cre* mice. B, Southern blot analysis of WT, *Cdh13<sup>fl/fl</sup>*, *Cdh13<sup>fl/fl</sup>* mice. C, PCR genotyping analysis of WT, *Cdh13<sup>fl/fl</sup>*, *Cdh13<sup>fl/fl</sup>* mice. D-F, *GlyT2::Cre*-mediated recombination occurs in mGluR2<sup>+</sup> (red arrows; D, E), Neurogranin<sup>+</sup> (yellow arrows; D, F) and mGluR2<sup>+</sup>Neurogranin<sup>+</sup> neurons (white arrows; D, E, F) of a P60 *GlyT2::Cre; Rosa::lox-stop-lox-eYFP* mouse. Some of Purkinje cells are indicated by asterisks. G-H, *Cdh13* expression is found in the IGL of the cerebellum of a P100 control mouse (I), but not in a P120 *GlyT2-Cdh13<sup>-/-</sup>* mouse (J). Corresponding area (Gi-Giii and Hi-Hiii) from control and *GlyT2-Cdh13<sup>-/-</sup>* mouse (red boxes in G, H). Scale bar = 100 μm (D-E), 1000 μm (G, H), 100 μm (Gi-Giii, Hi-Hiii)

detected at E14 (Figure S2). We next crossed *GlyT2::Cre* mice with *Cdh13<sup>fl/fl</sup>* mice to generate *GlyT2-Cdh13<sup>-/-</sup>* mice. We observed that ~85% of neurons in the IGL that express Neurogranin, a molecular marker expressed by most Golgi cells,<sup>55</sup> can be targeted by *GlyT2::Cre* mice (Figure 2G,H; Table S1). In addition, we found a >90% reduction in *Cdh13*<sup>+</sup> neurons in the IGL (Figure 2G,H; Table S1). Because ~83% of GAD67<sup>+</sup>-interneurons in the IGL normally express *Cdh13* (Table S1), our strategy permits the genetic manipulation of a majority, but not all presumptive Golgi cells.

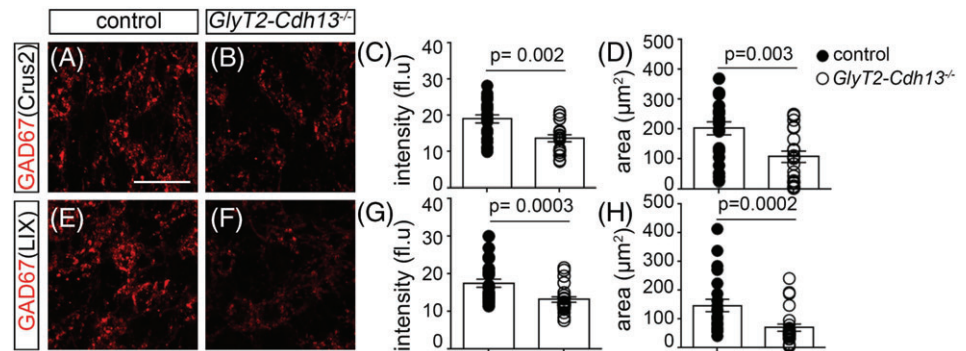
In addition to the cerebellum, analysis of regions where *Cdh13* is normally expressed and regions where *GlyT2::Cre*-mediated recombination takes place shows that *Cdh13* expression is preserved in most of the regions examined, but reduced in a subregion of the piriform cortex in *GlyT2-Cdh13<sup>-/-</sup>* mice (Figures S4 and S5; Table S1). We assessed the colocalization pattern of *Cdh13* and YFP in *GlyT2::Cre* recombined neurons in 4 brain regions that normally express *Cdh13* and are targeted by *GlyT2::Cre*-mediated recombination (Figure S3). Similar to our chromogenic *in situ* hybridization analysis (Figure S4), significant colocalization between *Cdh13* and YFP was detected in

*GlyT2::Cre* recombined neurons in the Pir and D/IE n indicating deletion of *Cdh13* occurred in these regions. Although we provide evidence that *Cdh13* expression is lost in select regions of the brain in *GlyT2-Cdh13<sup>-/-</sup>* mice, we have not been able to determine the extent of protein loss due to the lack of a reliable *Cdh13* antibody.

### 3.2 | Loss of *Cdh13* disrupts inhibitory synaptic protein expression/localization and electrophysiological properties of Golgi cells

*Cdh13* has been implicated in the organization of axon projections and the regulation of both excitatory and inhibitory synaptic functions.<sup>24,25,27</sup> To determine the functional relevance of *Cdh13* and whether loss of *Cdh13* in Golgi cells influences presynaptic function, we assessed the expression of GAD67 in the IGL of the cerebellar cortex which is derived primarily from Golgi cells.<sup>55</sup> We compared the intensity and area of GAD67 expression in *GlyT2-Cdh13<sup>-/-</sup>* and control mice in 2 lobules of the cerebellum (Figure 3A,B,E,F). In both Crus2 and lobule IX, the intensity of GAD67 expression is reduced by

**FIGURE 3** Loss of *Cdh13* results in reduction of the expression/localization of GAD67. A, B, E, F, Immunohistochemical analysis of the expression of GAD67 in the IGL of Crus2 and lobule IX in the cerebellum of control (A, E) and *GlyT2-Cdh13*<sup>-/-</sup> mice (P75-90) (B, F). C, G, Quantification of the intensity of GAD67 in Crus 2 and lobule IX (Crus2: control = 19.09 ± 1.14, *GlyT2-Cdh13*<sup>-/-</sup> = 13.7 ± 0.99, *U* = 99, *P* = .002, Mann-Whitney *U* test, *N* = 3, *n* = 20-22; LIX: control = 17.55 ± 1.08, *GlyT2-Cdh13*<sup>-/-</sup> = 13.2 ± 0.72, *U* = 103, *P* = .0003, Mann-Whitney *U* test, *N* = 3, *n* = 22-24). D, H, Quantification of the area coverage of GAD67 in Crus 2 and lobule IX (Crus2: control = 202.9 ± 21.87, *GlyT2-Cdh13*<sup>-/-</sup> = 107.5 ± 19.04, *U* = 103, *P* = .003, Mann-Whitney *U* test, *N* = 3, *n* = 20-22; LIX: control = 147.3 ± 21.42, *GlyT2-Cdh13*<sup>-/-</sup> = 70.3 ± 12.5, *U* = 100, *P* = .0002, Mann-Whitney *U* test, *N* = 3, *n* = 22-24). Closed circles: control, open circles: *GlyT2-Cdh13*<sup>-/-</sup>. Scale bar = 20 μm



~26% to 30% and area is reduced by ~47% to 49% in *GlyT2-Cdh13*<sup>-/-</sup> mice, compared to control (Figure 3C,D,G,H). The decrease in GAD67 expression is not a consequence of a reduction in the number of Golgi cells in *GlyT2-Cdh13*<sup>-/-</sup> mice due to potential specification or migration deficits (Figure S3; Table S2). The significant, but not total loss of the expression of GAD67 could be due to an incomplete deletion of *Cdh13* in IGL interneurons (Figure S1; Table 1), or partial deletion of *Cdh13* within individual neurons. These results indicate that *Cdh13* expression is required for proper expression and/or localization of GAD67, and suggests possible decrease in inhibitory activity in the cerebellum of *GlyT2-Cdh13*<sup>-/-</sup> mice.

Golgi cells receive excitatory input from granule cells and mossy fibers, as well as inhibitory input from Lugaro cells and other Golgi cells.<sup>13</sup> To assess whether loss of *Cdh13* perturbs the postsynaptic response of Golgi cells to these inputs, in addition to disruption of the expression/localization of GAD67, we performed whole-cell patch clamp measurements of postsynaptic responses of Golgi cells of *GlyT2-Cdh13*<sup>-/-</sup> mice (Figure 4A). To measure the spontaneous IPSCs (sIPSCs) in Golgi cells, we blocked the activity of AMPA receptors with NBQX and NMDA receptors with D-AP5.<sup>57</sup> We observed a decrease in the frequency of sIPSCs in Golgi cells of *GlyT2-Cdh13*<sup>-/-</sup> mice (Figure 4B,C), but not the amplitude of sIPSCs (Figure 4B,E; Table S3).

To further analyze the characteristics of inhibitory synaptic current in Golgi cells lacking *Cdh13*, we measured miniature IPSCs (mIPSCs) in Golgi cells by blocking action potential evoked GABA release with TTX. Similar to sIPSCs, miniature IPSC (mIPSC) frequency, but not amplitude, was reduced in Golgi cells of *GlyT2-*

*Cdh13*<sup>-/-</sup> mice (Figure 4B,D,F; Table S3). TTX treatment did not obviously affect the frequency or amplitude of IPSCs of Golgi cells, in both control and *GlyT2-Cdh13*<sup>-/-</sup> mice. We next recorded spontaneous EPSCs (sEPSCs) and miniature EPSCs (mEPSCs) by applying SR95531, a GABA<sub>A</sub> receptor antagonist, and strychnine, an antagonist of glycine receptors.<sup>58</sup> We found no differences in either sEPSC or mEPSC frequency, or amplitude of Golgi cells in control and *GlyT2-Cdh13*<sup>-/-</sup> mice (Figure 4B,G-J; Table S3). In brief, we observed changes in mIPSCs, but not mEPSCs of Golgi cells in *GlyT2-Cdh13*<sup>-/-</sup> mice. This indicates a selective reduction in the strength or number of inhibitory synapses, but not excitatory synapses, formed onto Golgi cells. Because Golgi cells form both feedforward and feedback inhibitory loops with granule cells to coordinate signal processing between mossy fibers and granule cells,<sup>13</sup> these impairments indicate that loss of *Cdh13* in Golgi cells perturbs the activity of Golgi cells, which may disrupt the cerebellar inhibitory network.

### 3.3 | Loss of *Cdh13* in cerebellar Golgi cells does not disrupt general locomotor activity

Immunotoxin ablation of Golgi cells in the cerebellum in mice results in severe motor dysfunction and ataxic phenotypes.<sup>14</sup> To assess the motor consequences of genetic manipulation rather than elimination of Golgi cells, we subjected *GlyT2-Cdh13*<sup>-/-</sup> mice to a series of motor behavioral paradigms. We examined their gross motor function using a rota-rod with an accelerating speed from 4 to 40 rotations per minute. *GlyT2-Cdh13*<sup>-/-</sup> mice learned the motor task at a level comparable to that of control mice (Figure 5A; Table S4). We also examined

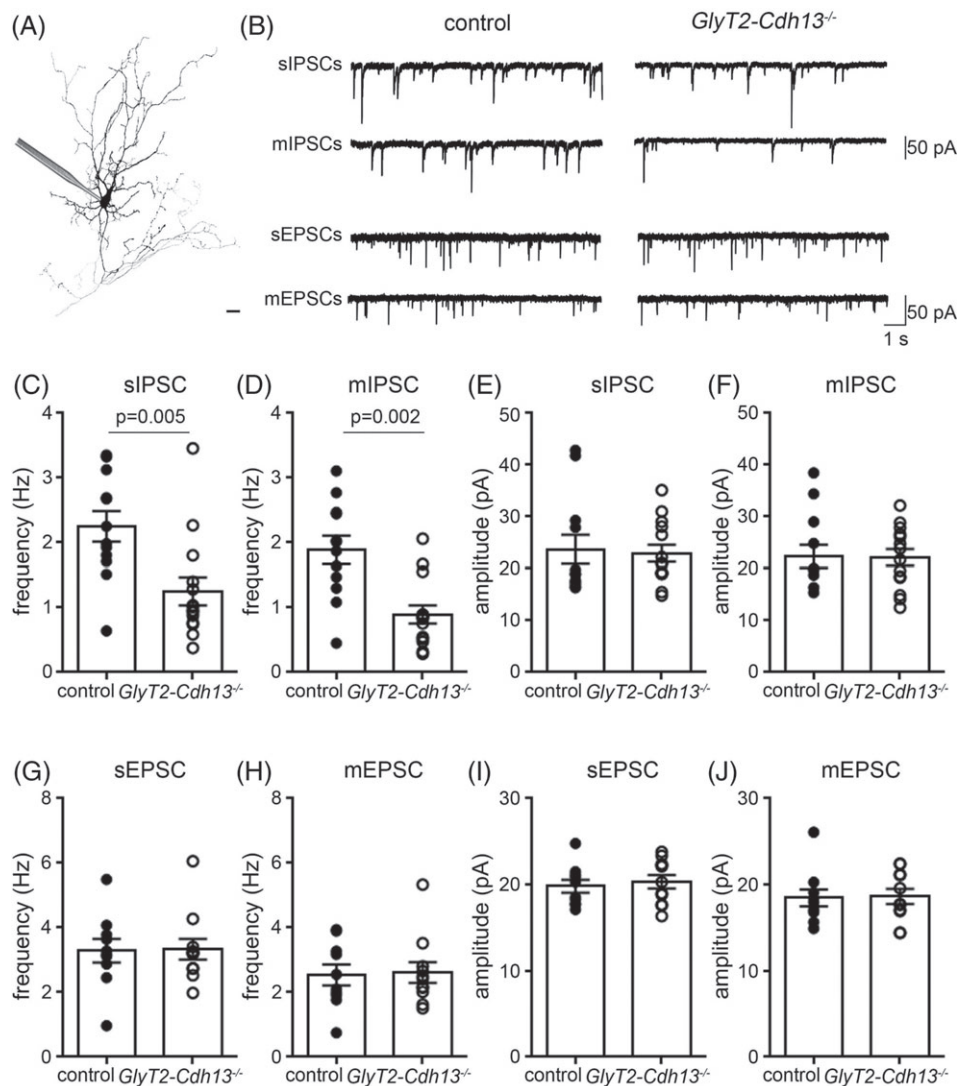


**FIGURE 4** Loss of *Cdh13* impairs postsynaptic responses of Golgi cells. A, Whole-cell patch clamp recording of Golgi cells in the IGL labeled with Neurobiotin. B, Examples of traces of spontaneous postsynaptic currents and miniature postsynaptic currents of Golgi cells in control and *GlyT2-Cdh13*<sup>-/-</sup> mice (P26-35). C-F, Analysis of inhibitory postsynaptic current of Golgi cells in the IGL of control and *GlyT2-Cdh13*<sup>-/-</sup> mice shows reduced sIPSC frequency (C,  $P = .005$ , Mann-Whitney  $U$  test) and decreased mIPSC frequency of *GlyT2-Cdh13*<sup>-/-</sup> Golgi cells compared to control (D,  $P = .002$ , Mann-Whitney  $U$  test). No differences in amplitude of both sIPSC and mIPSC were found between control and *GlyT2-Cdh13*<sup>-/-</sup> Golgi cells (sIPSC amplitude,  $P = .5$  Mann-Whitney  $U$  test; mIPSC amplitude  $P = 1.0$  Mann-Whitney  $U$  test) (E, F). G-J, Excitatory postsynaptic current in control and *GlyT2-Cdh13*<sup>-/-</sup> Golgi cells. sEPSC frequency and amplitude did not change in *GlyT2-Cdh13*<sup>-/-</sup> Golgi cells compared to control (G, I, sEPSC frequency  $P = .9$ , Mann-Whitney  $U$  test; sEPSC amplitude  $P = .6$  Mann-Whitney  $U$  test). In *GlyT2-Cdh13*<sup>-/-</sup> Golgi cells, both amplitude and frequency of mEPSC were not different from that of control Golgi cells (H, J, mEPSC frequency  $P = 1.0$  Mann-Whitney  $U$  test; mEPSC amplitude  $P = .9$  Mann-Whitney  $U$  test). Data presented as mean  $\pm$  SEM. P26-35 mice,  $n = 10-14$ /group. Scale bar = 20  $\mu$ m. See Table S3

the footprint pattern of *GlyT2-Cdh13*<sup>-/-</sup> and control mice in order to capture any subtle abnormalities in motor coordination associated with the loss of *Cdh13*. We observed that when walking freely in a walkway optimized for analysis of gait, *GlyT2-Cdh13*<sup>-/-</sup> mice walked with a tendency toward shorter strides, although this result did not reach statistical significance (Figure 5B,C; Table S4). Taken together, in contrast to a previous study showing severe motor dysfunction upon immunotoxin ablation of Golgi cells,<sup>14</sup> loss of *Cdh13* in Golgi cells does not lead to prominent motor phenotypes.

We next assessed the effects of conditional *Cdh13* deletion on spontaneous activity and novelty-induced anxiety in the open field. In addition, we examined whether *Cdh13* deletion results in

hyperactivity reported in mice with global loss of *Cdh13*.<sup>25</sup> During 7 minutes of free locomotion, *GlyT2-Cdh13*<sup>-/-</sup> mice traveled similar distances and at the same speed as control mice indicating comparable activity levels (Figure 5D-F; Table S4). To assess novelty-induced anxiety, we compared the duration of stay in the center vs corner zone of the open field as well as the number of visits to the center zone. *GlyT2-Cdh13*<sup>-/-</sup> mice behaved in a similar manner as control mice (Figure 5F-H; Table S4). Using a marble burying and digging paradigm, we examined the repetitive and perseverative behavior which has been shown to be a species-typical behavior sensitive to genetic manipulations.<sup>59</sup> *GlyT2-Cdh13*<sup>-/-</sup> and control mice buried a comparable number of marbles, indicating similar digging behavior (Figure 5I;

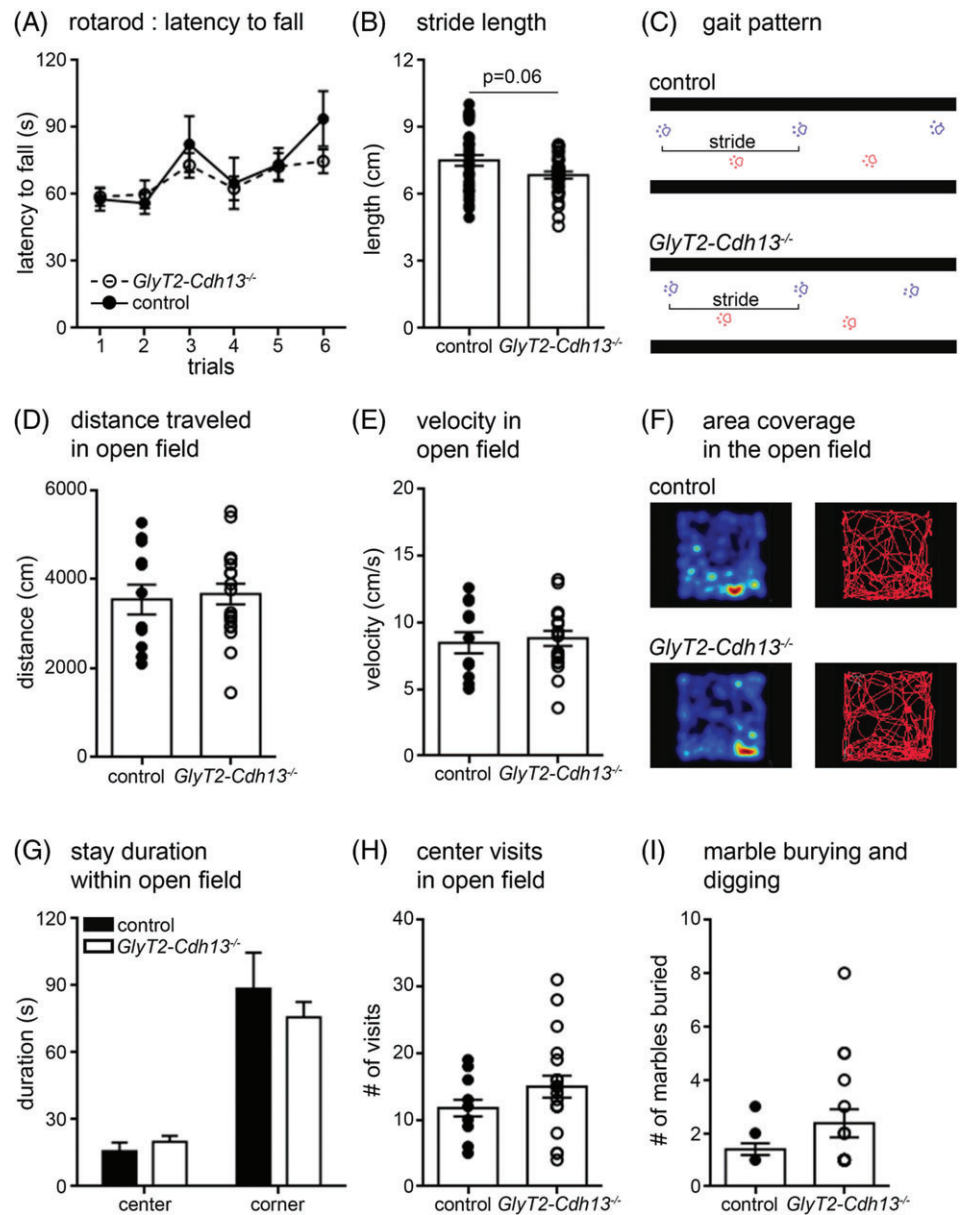


**FIGURE 5** Deletion of *Cdh13* in the cerebellum has no impact on general activity and motor coordination. A, In multiple trials on a rotating rod, *GlyT2-Cdh13*<sup>-/-</sup> mice display similar performance to that of control mice. B, *GlyT2-Cdh13*<sup>-/-</sup> mice show a tendency of making shorter strides during walking ( $P = .06$ , Mann-Whitney  $U$  test). C, Comparison of foot prints between control and *GlyT2-Cdh13*<sup>-/-</sup> mice. D, E, *GlyT2-Cdh13*<sup>-/-</sup> mice show comparable distance traveled (D) and velocity (E) during 7 minutes of free locomotion in an open arena. F, No genotype differences were detected in exploration of the open field as illustrated by the heat map of locomotion tracks. G, Open field anxiety-related readouts revealed no genotype differences in preference for corner/peripheral zone or center zone. H, Analysis of the number of visits to the center zone of the open field. I, Digging behavior was not influenced by *Cdh13* deletion. Data presented as mean  $\pm$  SEM. Adult male mice,  $n = 10$ -19/group. See Table S4

Table S4). Taken together, our results show that the absence of *Cdh13* in cerebellar Golgi cells did not have an impact on general motor coordination, locomotion or result in anxiety-like behaviors. However, we note here that the absence of gross motor-related phenotype could be due to the deletion of *Cdh13* in most, but not all IGL interneurons.

### 3.4 | Overtraining in 2-choice digging task reveals loss of cognitive flexibility in *GlyT2-Cdh13*<sup>-/-</sup> mice

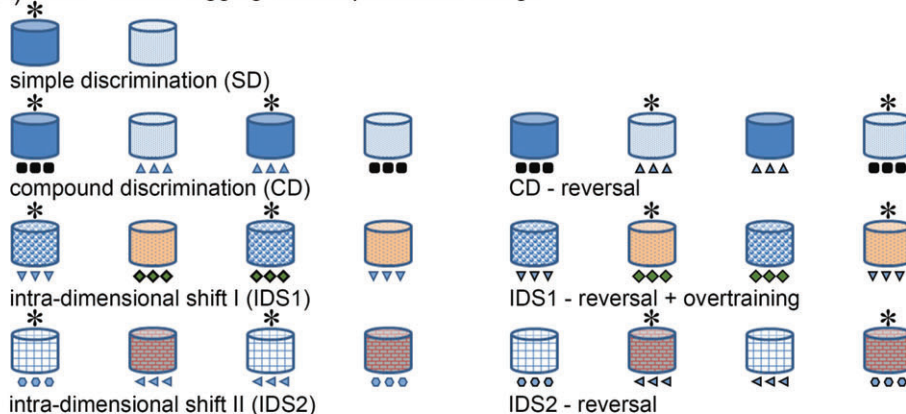
Cognitive flexibility is defined as the ability to adapt and shift from previously learned responses, and recent studies have shown that this behavior is not exclusively regulated by the prefrontal lobe.<sup>60,61</sup> Despite growing evidence linking the cerebellum with cognitive functions and behavioral disorders, our understanding of how disruption in candidate genes for ASD and ADHD, such as *Cdh13*, in specific cerebellar cell subtypes remains limited. Here, we aimed to assess the role of cerebellar Golgi cells in cognitive flexibility during discrimination

learning of a 2-choice digging task and to study whether the conditional deletion of *Cdh13* contributes to cognitive performance.

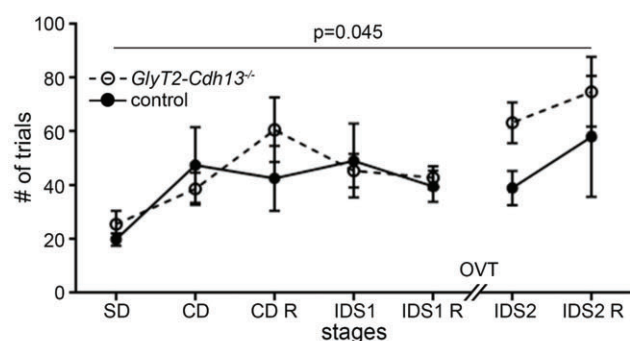
The 2-choice digging task is modeled and adapted from the Wisconsin card sorting test (WCST) administered to human subjects and the intradimensional/extradimensional set shifting task used in rodents.<sup>45-47</sup> *GlyT2-Cdh13*<sup>-/-</sup> and control mice were trained to perform a series of discriminations comprised of a simple and compound discrimination and reversal, an intradimensional shift and reversal, followed by an overtraining paradigm before another set of intradimensional shifts and reversals was introduced (Figure 6A). The task presents a series of discrimination challenges, in which mice are trained to associate a particular stimulus dimension with food reward. All mice tested readily acquired and performed a series of discrimination learning in the 2-choice digging task. However, we observed that *GlyT2-Cdh13*<sup>-/-</sup> mice show a lower level of performance (Figure 6B; Table S5).

To pose an additional cognitive challenge, we introduced mice to a new set of stimuli of the same dimensions after overtraining. Analysis of all completed trials before and after overtraining reveals

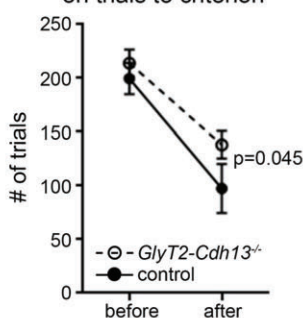
## (A) two – choice digging task: experimental design



## (B) trials to criterion across all stages



## (C) effects of overtraining on trials to criterion



## (D) effects of overtraining on performance errors

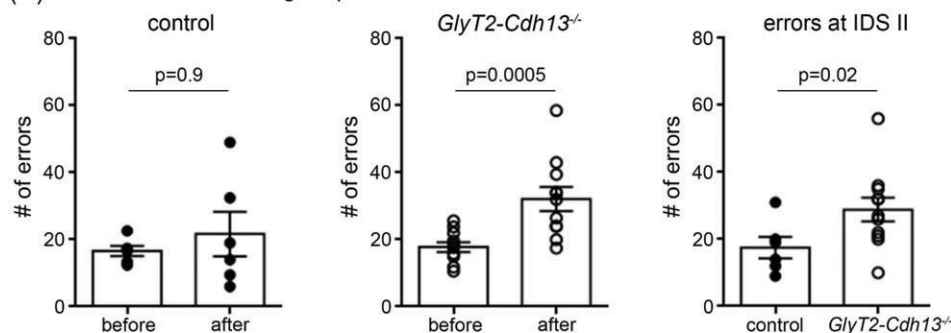


**FIGURE 6** Overtraining in 2-choice digging task reveals deficit in cognitive flexibility in *GlyT2-Cdh13<sup>-/-</sup>* mice. **A**, Experimental design and set of stimuli presented in the 2-choice digging task: the texture of the outer bowl as the relevant dimension that gave cue for the reward, while the type of the digging media was the irrelevant dimension. **B**, Both experimental groups were able to complete all 7 stages of the task, however *GlyT2-Cdh13<sup>-/-</sup>* mice need more trials to complete the task (2-way ANOVA, genotype  $P = .045$ , task  $P = .01$ ; genotype  $\times$  task  $P = .7$ ). **C**, Cumulative performance across all stages before and after overtraining showing higher number of cumulative trials of *GlyT2-Cdh13<sup>-/-</sup>* mice compared to control mice (2-way ANOVA, genotype  $P = .0453$ , task  $P = .0002$ ; genotype  $\times$  task  $P = .5$ ). **D**, Effects of overtraining on cognitive performance, measured in terms of errors made to reach criterion: average of performance errors of control (left graph: control mice,  $P = .9$ , Mann-Whitney  $U$  test) and *GlyT2-Cdh13<sup>-/-</sup>* mice (middle graph: *GlyT2-Cdh13<sup>-/-</sup>*,  $P = .0005$ , Mann-Whitney  $U$  test) prior to and after overtraining and *GlyT2-Cdh13<sup>-/-</sup>* mice made more errors at IDS 2 stage, commenced directly after overtraining (right graph:  $P = .02$ , Mann-Whitney  $U$  test). Data presented as mean  $\pm$  SEM. Adult male mice,  $n = 6-11$  per group. See Table S5

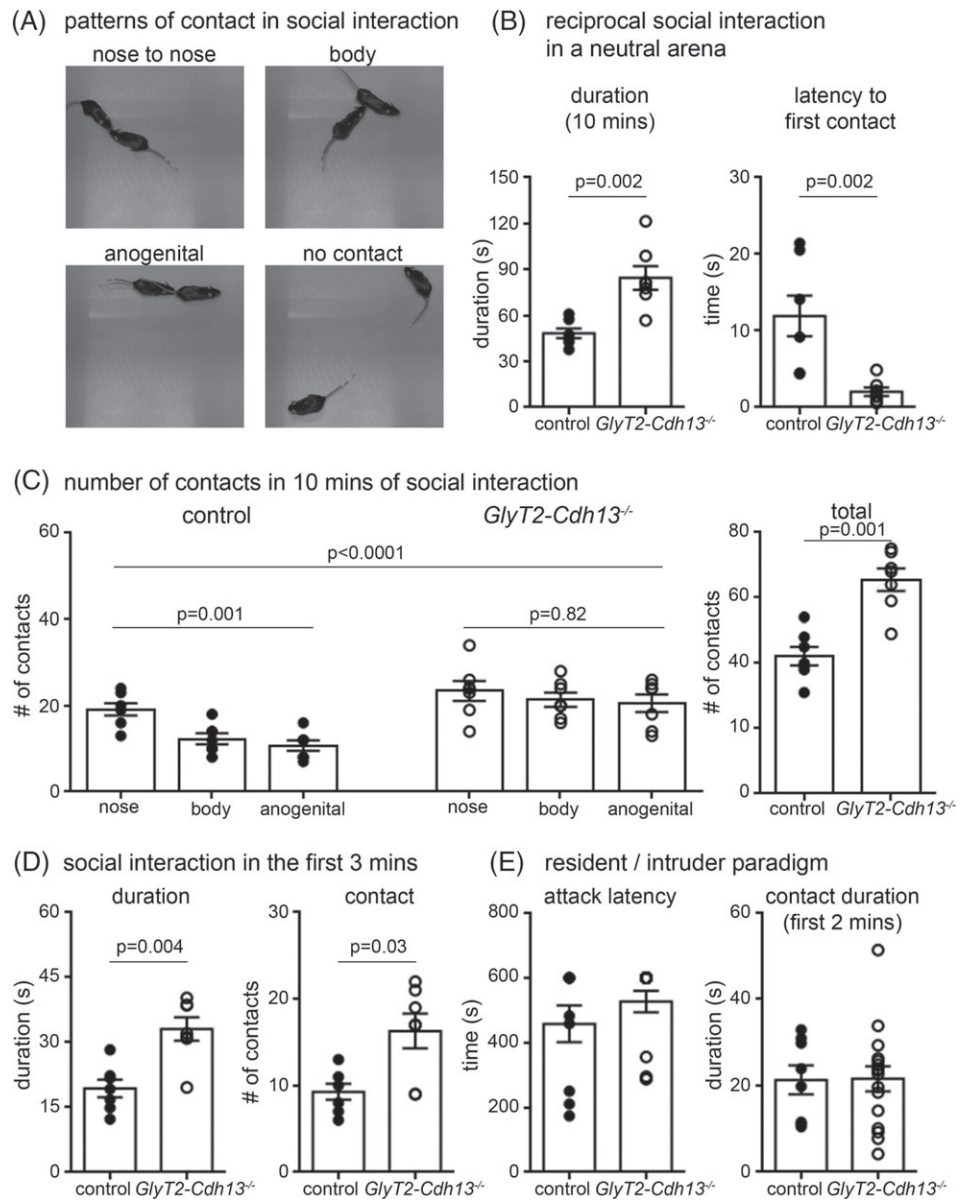
higher number of trials to criterion in *GlyT2-Cdh13<sup>-/-</sup>* mice (Figure 6C; Table 5). Similarly, overtraining also affected the performance of *GlyT2-Cdh13<sup>-/-</sup>* in terms of the average number of errors made to reach criterion (Figure 6D; Table S5). No difference was observed in the control group with respect to the average of errors made in all stages before and after overtraining, while *GlyT2-Cdh13<sup>-/-</sup>* mice made more errors (Figure 6D, control, *GlyT2-Cdh13<sup>-/-</sup>*; Table S5). Indeed, when a new set of stimuli was introduced after overtraining, *GlyT2-Cdh13<sup>-/-</sup>* mice made significantly more incorrect choices during trials of IDS2 (Figure 6D, errors at IDS II; Table S5). Taken together, these findings suggest that the interruption during a series of discrimination learning in forms of repeated and over exposure to a set of paired stimuli results in the decline of cognitive performance of *GlyT2-Cdh13<sup>-/-</sup>* mice. This phenotype appears more closely associated with the lack of cognitive flexibility, rather than a deficit in discrimination learning or the execution of the learned responses.

### 3.5 | Reciprocal social interaction is disrupted in *GlyT2-Cdh13<sup>-/-</sup>* mice

There is emerging evidence supporting a contribution of the cerebellum to social behaviors.<sup>5</sup> Deletion of *Tsc1*, *IB2* and *SHANK2* results in autistic-like behaviors, which includes aberrant social interaction in mice.<sup>9,62,63</sup> A genome-wide association study has linked *Cdh13* to extreme violence.<sup>34</sup> However, the role of cerebellar Golgi cells in regulating social behavior in animal models is not known. To investigate whether loss of *Cdh13* in the cerebellum influences social behavior, we tested *GlyT2-Cdh13<sup>-/-</sup>* mice for reciprocal social interaction in a novel and neutral environment, and a resident intruder paradigm for intermale aggression in a territorial environment.

During the free interaction of reciprocal social interaction, we scored and observed the pattern of social interaction, which included nose-to-nose, nose-to-body and nose-to-anogenital area contacts (Figure 7A). Pairs of *GlyT2-Cdh13<sup>-/-</sup>* mice stayed almost twice as long

**FIGURE 7** *GlyT2-Cdh13*<sup>-/-</sup> mice exhibit increase in reciprocal social interactions with loss of preference for contact region. A, Pattern of contacts during 10 minutes of reciprocal social interaction in a novel arena of same pair genotype: nose-nose, nose-body and nose-anogenital area. B, During 10 minutes of social interaction, pairs of *GlyT2-Cdh13*<sup>-/-</sup> mice display a cumulative preference to be in contact ( $P = .002$ , Mann-Whitney *U* test) and took a shorter time to initiate contact ( $P = .0023$ , Mann-Whitney *U* test). C, Evaluation of the number of contacts to nose, body and anogenital area shows a preference for contact to nose in pairs of control mice ( $P = .001$ , Kruskal-Wallis test), but no preference for nose, body or anogenital in *GlyT2-Cdh13*<sup>-/-</sup> mice ( $P = .82$ , Mann-Whitney *U* test) despite an increase in number of total contacts (see Table S4). D, Analysis of the first 3 of 10 minutes of social interaction revealed increased in the duration ( $P = .004$ , Mann-Whitney *U* test) and number of contacts ( $P = .03$ , Mann-Whitney *U* test) made by *GlyT2-Cdh13*<sup>-/-</sup> mice. E, In the resident-intruder paradigm to assess for inter-male aggression, no genotype differences was observed in latency to attack and duration of contact, including following and sniffing behavior. Data presented as mean  $\pm$  SEM. Adult male mice,  $n = 10$ -16 per group. See Table S6



in contact with each other and exhibited latency to first contact ~6 times faster compared to pairs of control mice during 10-minute sessions of social interaction (Figure 7B; Video S1). We assessed the number of contacts and observed an increase of social contacts in pairs of *GlyT2-Cdh13*<sup>-/-</sup> mice (Figure 7C, total; Video S1; Table S6). Control mice displayed varied contact frequency to different body parts, with nose-to-nose contacts being the most frequent, followed by nose-to-body and nose-to anogenital (Figure 7C, control; Table S6). Interestingly, however, no such variance was seen in pairs of *GlyT2-Cdh13*<sup>-/-</sup> mice, despite a significant increase of total contacts observed in pairs of *GlyT2-Cdh13*<sup>-/-</sup> mice (Figure 7C, *GlyT2-Cdh13*<sup>-/-</sup>, total; Table S6).

To determine whether novelty influences social interaction, we analyzed the social interaction within the initial 3 minutes after 2 mice are placed in the arena. We found an increase in duration and number of contacts, indicating *GlyT2-Cdh13*<sup>-/-</sup> mice exhibit a preference for social contact during the initial 3 minutes of the interaction (Figure 7D; Table S6). In contrast to the results of the reciprocal social interaction test, we observed no genotype differences in the

resident-intruder paradigm to test for male aggression. The attack latency and contact duration during the first 2 minutes of resident *GlyT2-Cdh13*<sup>-/-</sup> mice were indistinguishable from that of control resident mice (Figure 7E, latency, duration; Table S6). Thus, we show that the conditional deletion of *Cdh13* disrupts social behavior in a selective manner depending on the social context. Tested in a neutral and novel arena, *GlyT2-Cdh13*<sup>-/-</sup> mice exhibit increased social interaction and investigations. However, in a territorial setting of the home cage, *GlyT2-Cdh13*<sup>-/-</sup> mice exhibited behavior comparable to that of control mice.

To assess whether *GlyT2-Cdh13*<sup>-/-</sup> mice exhibit pro-social behavior due to impairment in olfactory functions, we tested mice in odor habituation/dishabituation paradigm.<sup>44</sup> Both *GlyT2-Cdh13*<sup>-/-</sup> and control mice show discriminative responses toward social and nonsocial odors (Figure S4; Table S6). Both mice showed a habituated response to repeated presentation of an odor and dishabituation response to a novel odor (Figure S4; Table S6). These results indicate that lack of *Cdh13* in the cerebellum and the piriform cortex does not disrupt the olfactory responsiveness and discriminative response

toward both social and nonsocial odors, and that the social phenotype we observed in mice lacking *Cdh13* in Golgi cells might be related to disruptions in processing rather than recognition of social cue. Taken together, we show that *GlyT2-Cdh13*<sup>-/-</sup> mice exhibit increased social interaction accompanied by the loss of preference for a specific body zone during contact. While an increase of contacts in *GlyT2-Cdh13*<sup>-/-</sup> mice might suggest a pro-social phenotype, or increased social approach, the disappearance of preference for nose-to-nose contacts indicates abnormalities in social repertoire. Furthermore, the selective increase in social interaction in neutral and novel arenas, but not in territorial arena within a setting for agonistic interaction, suggests that the deletion of *Cdh13* in the cerebellum and the piriform cortex may have disrupted the processing of relevant social cues.

## 4 | DISCUSSION

The cerebellum mediates not only the precision and timing of movement, but also is implicated in nonmotor functions linked to ASD and ADHD.<sup>2,64,65</sup> However, the underlying mechanisms proposed for the regulation of nonmotor functions have been derived largely from analysis of Purkinje cells.<sup>61,62,66</sup> Because Golgi and Purkinje cells have been proposed to differentially process shared input,<sup>67</sup> assessment of the contribution of Golgi cells to nonmotor functions is essential. Selective ablation of Golgi cells results in severe motor dysfunctions in mice and therefore precludes analysis of cognitive and social behaviors.<sup>14</sup> Here, we show that the deletion of *Cdh13* in select neuronal subpopulations, including cerebellar Golgi cells, and perturbation of their function without elimination of these neurons, preserved general motor functions in *GlyT2-Cdh13*<sup>-/-</sup> mice. Although our results cannot rule out the involvement of *Cdh13* in motor-related processes, we were afforded an opportunity to assess the behavioral consequences without disruption in motor coordination/learning and general locomotor activity. We discuss how *Cdh13* regulates inhibitory synaptic function and how perturbation of the cerebellar inhibitory network may have overt effects on cognitive and social behaviors.

### 4.1 | *Cdh13* as a genetic entry point to examine the involvement of Golgi cells in mediating cerebellar-related behaviors

*Cdh13*, a gene that has been implicated in ASD and aggressive behaviors,<sup>33,34</sup> is emerging as a key regulator of neuronal functions, including migration, axon targeting and synapse formation.<sup>24,25,27-29</sup> Functional-structure analysis of *Cdh13* has revealed insight as to how *Cdh13* is able to achieve these diverse functions.<sup>68-70</sup> *Cdh13* is an atypical cadherin that has 5 preserved extracellular domains, but lacks transmembrane and intracellular domains.<sup>71,72</sup> Similar to classical cadherins, *Cdh13* exerts its activities through homophilic interactions with an extracellular domain and intermembrane interactions with a glycosyl-phosphatidylinositol anchor.<sup>71,73</sup> In addition, through interactions with proteins containing intracellular constituents, such as GABA<sub>A</sub> receptors and integrins, *Cdh13* has the ability to influence many signaling cascades.<sup>68,70,74,75</sup> The complexities and intricacies of

*Cdh13* activities raise the importance of systematically investigating specific brain regions and neuronal subtypes that express *Cdh13*.

Previous studies exploring the function of *Cdh13* have assessed mice with wholesale deletion of *Cdh13*.<sup>25,26</sup> Although these studies linked *Cdh13* with GABAergic function in the hippocampus and cognitive processes,<sup>25</sup> and with dopaminergic signaling in the cortex and addiction,<sup>26</sup> their approach precludes the ability to examine involvement of the precise brain region or neuronal subpopulation which expresses *Cdh13*. The selective expression of *Cdh13* in Golgi cells and our strategy to delete *Cdh13* in Golgi cells using *GlyT2::Cre* mice provide a means to study the function of *Cdh13* in a more restricted manner. Importantly, this strategy offers an opportunity to examine the role of Golgi cells in mediating behavioral processes, which has been a challenging task due to the lack of genetic tools to selectively manipulate their gene expression or function. Our strategy, however, only permits the genetic manipulation of a majority of presumptive Golgi cells, raising the possibility that the manipulation of this entire neuronal subpopulation may result in more pronounced behavioral deficits. Another limitation of our strategy is that although *GlyT2::Cre* mice mediates recombination in Golgi cells, recombination does occur in some Purkinje and stellate/basket cells (Figure 2D).<sup>35</sup> In addition to *Cdh13*, many genes implicated in ASD or schizophrenia, such as *Tsc1*, *Cntnap4*, *Cntnap2* and *Shank3* are expressed in Golgi cells (Allen Brain Atlas). Thus, the development of a novel strategy to delete these genes selectively in Golgi cells may reveal insight about the function of Golgi cells as well as the link between perturbation in Golgi cell function and neurological disorders.

### 4.2 | Contribution of the cerebellum to cognitive flexibility

The cerebellum has been proposed to influence executive functions that require cognitive flexibility.<sup>60,61</sup> In a touch screen-based task, mice with Purkinje cell loss show impairment of reversal learning and extradimensional (ED) set shifting.<sup>61</sup> Also, hemi-cerebellectomized rats perform poorly in the final phases of a task designed to measure cognitive flexibility.<sup>60</sup> In the 2-choice digging task, we assess the cognitive flexibility of mice with disrupted cerebellar Golgi cells to perform a series of discrimination learning task in response to a set of stimuli presented.<sup>46</sup> Only after confronted with a series of overtraining to reinforce the same set of stimuli, *GlyT2-Cdh13*<sup>-/-</sup> mice perform poorly compared to control mice at the subsequent stages, despite within-dimension (intradimensional) changes of stimuli set. Additional presentation of the same dimensions has been shown to strengthen the formation of attentional set,<sup>45,47</sup> which may have contributed to the poor performance observed in *GlyT2-Cdh13*<sup>-/-</sup> mice at the stages after overtraining.

Cerebellar dysfunction has been implicated in ASD,<sup>2,5</sup> and disturbances in cognitive flexibility have been associated with both the cerebellum and ASD.<sup>76</sup> Set shifting deficits have been reported to be an intermediate phenotype for ASD, but a majority of studies have failed to distinguish ASD from typical developing children,<sup>77,78</sup> and results from intradimensional/extradimensional (IDED) task are often conflicting.<sup>79,80</sup> For instance, while typical ASD individuals have difficulty during ED, but not ID shift,<sup>81</sup> high functioning ASD children have

difficulty in ID, but not ED shifts.<sup>82</sup> In a study using IDED task, ASD children have more difficulty at later and cognitively more complex stages of set shifting tasks.<sup>80</sup> Using an adapted version of the task, without extradimensional shifts, we show that *GlyT2-Cdh13*<sup>-/-</sup> mice follow a similar pattern and the deficits manifest only at later stages after overtraining. Taken together, our results and those from human studies suggest that disruptions in the cerebellum influence the ability to adapt to changes following the manipulation of otherwise regular patterns of discrimination learning (ie, after over-exposure of a certain set of stimulus pairs), rather than in the initial acquisition of discrimination learning.

### 4.3 | Cerebellar network and atypical social interaction

Ablation of *Cdh13* expression in Golgi cells leads to a surprising result, where *GlyT2-Cdh13*<sup>-/-</sup> mice display atypical increases of reciprocal social interactions, but with a disappearance of the preference for nose-to-nose contacts. Unlike pairs of control mice that display an obvious preference for facial contacts compared to body and anogenital contacts, *GlyT2-Cdh13*<sup>-/-</sup> mice show equal number of contacts to facial, body and anogenital area. Reduced nose-to-nose sniffing in mice during social interaction has been proposed to be analogous to reduced eye contact observed in ASD individuals.<sup>83</sup> The absence of preference for a specific body part in *GlyT2-Cdh13*<sup>-/-</sup> mice is reminiscent of symptoms exhibited by ASD individuals and could arise from deficits in olfactory processing. The piriform cortex has been shown to be critical for odorant recognition and processing,<sup>84,85</sup> and thus the atypical social interaction we observed could, in principle, be a consequence of *Cdh13* deletion in the piriform cortex and cerebellum. Interestingly, in humans, the piriform cortex and the cerebellum have been shown to contribute to odor recognition memory and odor intensity/quality discrimination, respectively.<sup>86</sup> Our result in mice indicates that the genetic manipulation of neuronal subpopulations in both regions could disrupt odorant recognition which could lead to social interaction deficits.

Atypical and increased social interactions have been linked to the disruption of granule cells in *CD47* knock-out mice.<sup>87</sup> The deletion of *Tsc1*, *IB2*, and an autism-related gene *SHANK2* in Purkinje cells results in an autistic-like phenotype, which includes aberrant social interaction in mice.<sup>9,62,63</sup> Besides Purkinje cells, studies on other components of the cerebellar network, such as Golgi cells, and how they might influence social interaction are lacking. In principle, in addition to Purkinje cell deficits, disruptions to Golgi cell function could also cause behavioral deficits including abnormal social interaction, since they are linked to Purkinje cells. The observation that mice lacking *Cdh13* in Golgi cells exhibit disrupted social interaction in a novel and neutral setting, therefore, suggests that perturbation in Golgi cell function may be an important contributing factor in behavioral deficits associated with neurological disorders.

### ACKNOWLEDGMENTS

We thank Ong Yee Hwee and Alaric Yip for technical assistance. J. Nicholas Betley, Toh Hean Ch'ng and Ayumu Tashiro provided

discussion and comments on the manuscript. Work was supported by a Cooperative Basic Research Grant from the Singapore National Medical Research Council (NMRC/CBRG/0075/2014) and Tier 1 award from the Singapore Ministry of Education (RG124/15).

### Conflict of interest

The authors declare no potential conflict of interests.

### ORCID

A. I. Chen  <http://orcid.org/0000-0001-5355-024X>

### REFERENCES

- Ito M. Cerebellar circuitry as a neuronal machine. *Prog Neurobiol.* 2006;78:272-303.
- Reeber SL, Otis TS, Sillitoe RV. New roles for the cerebellum in health and disease. *Front Syst Neurosci.* 2013;7:83.
- Berquin PC, Giedd JN, Jacobsen LK, et al. Cerebellum in attention-deficit hyperactivity disorder: a morphometric MRI study. *Neurology.* 1998;50:1087-1093.
- Mostofsky SH, Mazzocco MM, Aakalu G, Warsofsky IS, Denckla MB, Reiss AL. Decreased cerebellar posterior vermis size in fragile X syndrome: correlation with neurocognitive performance. *Neurology.* 1998;50:121-130.
- Rogers TD, McKimm E, Dickson PE, Goldowitz D, Blaha CD, Mittleman G. Is autism a disease of the cerebellum? An integration of clinical and pre-clinical research. *Front Syst Neurosci.* 2013;7:15.
- Wang SS, Klothe AD, Badura A. The cerebellum, sensitive periods, and autism. *Neuron.* 2014;83:518-532.
- Sudarov A. Defining the role of cerebellar Purkinje cells in autism spectrum disorders. *Cerebellum.* 2013;12:950-955.
- Tran KD, Smutzer GS, Doty RL, Arnold SE. Reduced Purkinje cell size in the cerebellar vermis of elderly patients with schizophrenia. *Am J Psychiatry.* 1998;155:1288-1290.
- Tsai PT, Hull C, Chu Y, et al. Autistic-like behaviour and cerebellar dysfunction in Purkinje cell *Tsc1* mutant mice. *Nature.* 2012;488:647-651.
- Albus JS. A theory of cerebellar function. *Math Biosci.* 1971;10:25-61.
- Gabbiani F, Midtgaard J, Knopfel T. Synaptic integration in a model of cerebellar granule cells. *J Neurophysiol.* 1994;72:999-1009.
- Marr D. A theory of cerebellar cortex. *J Physiol.* 1969;202:437-470.
- D'Angelo E, Solinas S, Mapelli J, Gandolfi D, Mapelli L, Prestori F. The cerebellar Golgi cell and spatiotemporal organization of granular layer activity. *Front Neural Circuits.* 2013;7:93.
- Watanabe D, Inokawa H, Hashimoto K, et al. Ablation of cerebellar Golgi cells disrupts synaptic integration involving GABA inhibition and NMDA receptor activation in motor coordination. *Cell.* 1998;95:17-27.
- Kheradmand A, Zee DS. Cerebellum and ocular motor control. *Front Neurol.* 2011;2:53.
- Raymond JL. Learning in the oculomotor system: from molecules to behavior. *Curr Opin Neurobiol.* 1998;8:770-776.
- Kalmbach BE, Voicu H, Ohyama T, Mauk MD. A subtraction mechanism of temporal coding in cerebellar cortex. *J Neurosci.* 2011;31:2025-2034.
- Rossert C, Dean P, Porrill J. At the edge of chaos: how cerebellar granular layer network dynamics can provide the basis for temporal filters. *PLoS Comput Biol.* 2015;11:e1004515.
- Honjo M, Tanihara H, Suzuki S, Tanaka T, Honda Y, Takeichi M. Differential expression of cadherin adhesion receptors in neural retina of the postnatal mouse. *Invest Ophthalmol Vis Sci.* 2000;41:546-551.
- Price SR, De Marco Garcia NV, Ranscht B, Jessell TM. Regulation of motor neuron pool sorting by differential expression of type II cadherins. *Cell.* 2002;109:205-216.
- Redies C, Hertel N, Hubner CA. Cadherins and neuropsychiatric disorders. *Brain Res.* 2012;1470:130-144.

22. Yamagata M, Sanes JR, Weiner JA. Synaptic adhesion molecules. *Curr Opin Cell Biol.* 2003;15:621-632.
23. Zipursky SL, Sanes JR. Chemoaffinity revisited: dscams, protocadherins, and neural circuit assembly. *Cell.* 2010;143:343-353.
24. Paradis S, Harrar DB, Lin YX, et al. An RNAi-based approach identifies molecules required for glutamatergic and GABAergic synapse development. *Neuron.* 2007;53:217-232.
25. Rivero O, Selten MM, Sich S, et al. Cadherin-13, a risk gene for ADHD and comorbid disorders, impacts GABAergic function in hippocampus and cognition. *Transl Psychiatry.* 2015;5:e655.
26. Drgonova J, Walther D, Hartstein GL, et al. Cadherin 13: human cis-regulation and selectively-altered addiction phenotypes and cerebral cortical dopamine in knockout mice. *Mol Med.* 2016;22:1.
27. Hayano Y, Zhao H, Kobayashi H, Takeuchi K, Norioka S, Yamamoto N. The role of T-cadherin in axonal pathway formation in neocortical circuits. *Development.* 2014;141:4784-4793.
28. Killen AC, Barber M, Paulin JJ, Ranscht B, Parnavelas JG, Andrews WD. Protective role of Cadherin 13 in interneuron development. *Brain Struct Funct.* 2017;222:3567-3585.
29. Poliak S, Norovich AL, Yamagata M, Sanes JR, Jessell TM. Muscle-type identity of proprioceptors specified by spatially restricted signals from limb mesenchyme. *Cell.* 2016;164:512-525.
30. Fredette BJ, Miller J, Ranscht B. Inhibition of motor axon growth by T-cadherin substrata. *Development.* 1996;122:3163-3171.
31. Fredette BJ, Ranscht B. T-cadherin expression delineates specific regions of the developing motor axon-hindlimb projection pathway. *J Neurosci.* 1994;14:7331-7346.
32. Ranscht B, Bronner-Fraser M. T-cadherin expression alternates with migrating neural crest cells in the trunk of the avian embryo. *Development.* 1991;111:15-22.
33. Sanders SJ, Ercan-Sencicek AG, Hus V, et al. Multiple recurrent de novo CNVs, including duplications of the 7q11.23 Williams syndrome region, are strongly associated with autism. *Neuron.* 2011;70:863-885.
34. Tiihonen J, Rautiainen MR, Ollila HM, et al. Genetic background of extreme violent behavior. *Mol Psychiatry.* 2015;20:786-792.
35. Ishihara N, Armsen W, Papadopoulos T, Betz H, Eulenburg V. Generation of a mouse line expressing Cre recombinase in glycinergic interneurons. *Genesis.* 2010;48:437-445.
36. Srinivas S, Watanabe T, Lin CS, et al. Cre reporter strains produced by targeted insertion of EYFP and ECFP into the ROSA26 locus. *BMC Dev Biol.* 2001;1:4.
37. Schambra UB, Lauder JM, Silver J. *Atlas of the prenatal mouse brain.* San Diego: Academic Press; 1992.
38. Oliva AA Jr, Swann JW. Fluorescence in situ hybridization method for co-localization of mRNA and GEP. *Biotechniques.* 2001;31(74-76):78-81.
39. Schaeren-Wiemers N, Gerfin-Moser A. A single protocol to detect transcripts of various types and expression levels in neural tissue and cultured cells: in situ hybridization using digoxigenin-labelled cRNA probes. *Histochemistry.* 1993;100:431-440.
40. Vosshall LB, Amrein H, Morozov PS, Rzhetsky A, Axel R. A spatial map of olfactory receptor expression in the *Drosophila* antenna. *Cell.* 1999;96:725-736.
41. Kim J, Lee S, Tsuda S, et al. Optogenetic mapping of cerebellar inhibitory circuitry reveals spatially biased coordination of interneurons via electrical synapses. *Cell Rep.* 2014;7:1601-1613.
42. Kim H, Son J, Yoo H, et al. Effects of the female estrous cycle on the sexual behaviors and ultrasonic vocalizations of male C57BL/6 and autistic BTBR T+ tf/J Mice. *Exp Neurol.* 2016;25:156-162.
43. Meziane H, Ouagazzal AM, Aubert L, Wietrzyk M, Krezel W. Estrous cycle effects on behavior of C57BL/6J and BALB/cByJ female mice: implications for phenotyping strategies. *Genes Brain Behav.* 2007;6:192-200.
44. Arbuckle EP, Smith GD, Gomez MC, Lugo JN. Testing for Odor Discrimination and Habituation in Mice. *J. Vis. Exp.* 2015;(99):e52615. <https://doi.org/10.3791/52615>.
45. Bissonette GB, Martins GJ, Franz TM, Harper ES, Schoenbaum G, Powell EM. Double dissociation of the effects of medial and orbital prefrontal cortical lesions on attentional and affective shifts in mice. *J Neurosci.* 2008;28:11124-11130.
46. Chuang H, Huang T, Hsueh Y. Two-choice Digging Task in Mouse for Studying the Cognitive Flexibility. *Bio-protocol* 2014;4(19):e1250. <https://doi.org/10.21769/BioProtoc.1250>.
47. Garner JP, Thogerson CM, Wurler H, Murray JD, Mench JA. Animal neuropsychology: validation of the intra-dimensional extra-dimensional set shifting task for mice. *Behav Brain Res.* 2006;173:53-61.
48. Ashley S, Pearson J. When more equals less: overtraining inhibits perceptual learning owing to lack of wakeful consolidation. *Proc Biol Sci.* 2012;279:4143-4147.
49. Moy SS, Nadler JJ, Perez A, et al. Sociability and preference for social novelty in five inbred strains: an approach to assess autistic-like behavior in mice. *Genes Brain Behav.* 2004;3:287-302.
50. Machado AS, Darmohray DM, Fayad J, Marques HG, Carey MR. A quantitative framework for whole-body coordination reveals specific deficits in freely walking ataxic mice. *Elife.* 2015;4:e07892.
51. Mendes CS, Bartos I, Marka Z, Akay T, Marka S, Mann RS. Quantification of gait parameters in freely walking rodents. *BMC Biol.* 2015;13:50.
52. Rubina KA, Smutova VA, Semenova ML, et al. Detection of T-Cadherin expression in mouse embryos. *Acta Naturae.* 2015;7:87-94.
53. Esclapez M, Tillakaratne NJ, Kaufman DL, Tobin AJ, Houser CR. Comparative localization of two forms of glutamic acid decarboxylase and their mRNAs in rat brain supports the concept of functional differences between the forms. *J Neurosci.* 1994;14:1834-1855.
54. Leto K, Rolando C, Rossi F. The genesis of cerebellar GABAergic neurons: fate potential and specification mechanisms. *Front Neuroanat.* 2012;6:6.
55. Simat M, Parpan F, Fritschy JM. Heterogeneity of glycinergic and gabaergic interneurons in the granule cell layer of mouse cerebellum. *J Comp Neurol.* 2007;500:71-83.
56. Husson Z, Rousseau CV, Broll I, Zeilhofer HU, Dieudonne S. Differential GABAergic and glycinergic inputs of inhibitory interneurons and Purkinje cells to principal cells of the cerebellar nuclei. *J Neurosci.* 2014;34:9418-9431.
57. Micu I, Jiang Q, Coderre E, et al. NMDA receptors mediate calcium accumulation in myelin during chemical ischaemia. *Nature.* 2006;439:988-992.
58. Bieda MC, MacIver MB. Major role for tonic GABAA conductances in anesthetic suppression of intrinsic neuronal excitability. *J Neurophysiol.* 2004;92:1658-1667.
59. Deacon RM. Digging and marble burying in mice: simple methods for in vivo identification of biological impacts. *Nat Protoc.* 2006;1:122-124.
60. De Bartolo P, Mandolesi L, Federico F, et al. Cerebellar involvement in cognitive flexibility. *Neurobiol Learn Mem.* 2009;92:310-317.
61. Dickson PE, Cairns J, Goldowitz D, Mittleman G. Cerebellar contribution to higher and lower order rule learning and cognitive flexibility in mice. *Neuroscience.* 2017;345:99-109.
62. Giza J, Urbanski MJ, Prestori F, et al. Behavioral and cerebellar transmission deficits in mice lacking the autism-linked gene *islet brain-2*. *J Neurosci.* 2010;30:14805-14816.
63. Peter S, Ten Brinke MM, Stedehouder J, et al. Dysfunctional cerebellar Purkinje cells contribute to autism-like behaviour in Shank2-deficient mice. *Nat Commun.* 2016;7:12627.
64. Schmahmann JD. The role of the cerebellum in cognition and emotion: personal reflections since 1982 on the dysmetria of thought hypothesis, and its historical evolution from theory to therapy. *Neuropsychol Rev.* 2010;20:236-260.
65. Strick PL, Dum RP, Fiez JA. Cerebellum and nonmotor function. *Annu Rev Neurosci.* 2009;32:413-434.
66. Carter AG, Regehr WG. Quantal events shape cerebellar interneuron firing. *Nat Neurosci.* 2002;5:1309-1318.
67. Hull C, Regehr WG. Identification of an inhibitory circuit that regulates cerebellar Golgi cell activity. *Neuron.* 2012;73:149-158.
68. Philippova M, Joshi MB, Kyriakakis E, Pfaff D, Erne P, Resink TJ. A guide and guard: the many faces of T-cadherin. *Cell Signal.* 2009;21:1035-1044.

69. Ranscht B, Dours-Zimmermann MT. T-cadherin, a novel cadherin cell adhesion molecule in the nervous system lacks the conserved cytoplasmic region. *Neuron*. 1991;7:391-402.
70. Rivero O, Sich S, Popp S, Schmitt A, Franke B, Lesch KP. Impact of the ADHD-susceptibility gene CDH13 on development and function of brain networks. *Eur Neuropsychopharmacol*. 2013;23:492-507.
71. Ciatto C, Bahna F, Zampieri N, et al. T-cadherin structures reveal a novel adhesive binding mechanism. *Nat Struct Mol Biol*. 2010;17:339-347.
72. Hirano S, Suzuki ST, Redies C. The cadherin superfamily in neural development: diversity, function and interaction with other molecules. *Front Biosci*. 2003;8:d306-d355.
73. Vestal DJ, Ranscht B. Glycosyl phosphatidylinositol-anchored T-cadherin mediates calcium-dependent, homophilic cell adhesion. *J Cell Biol*. 1992;119:451-461.
74. Kyriakakis E, Maslova K, Frachet A, et al. Cross-talk between EGFR and T-cadherin: EGFR activation promotes T-cadherin localization to intercellular contacts. *Cell Signal*. 2013;25:1044-1053.
75. Um JW, Ko J. Neural glycosylphosphatidylinositol-anchored proteins in synaptic specification. *Trends Cell Biol*. 2017;27:931-945.
76. Ridley NJ, Homewood J, Walters J. Cerebellar dysfunction, cognitive flexibility and autistic traits in a non-clinical sample. *Autism*. 2011;15:728-745.
77. Goldberg MC, Mostofsky SH, Cutting LE, et al. Subtle executive impairment in children with autism and children with ADHD. *J Autism Dev Disord*. 2005;35:279-293.
78. Sinzig J, Morsch D, Bruning N, Schmidt MH, Lehmkuhl G. Inhibition, flexibility, working memory and planning in autism spectrum disorders with and without comorbid ADHD-symptoms. *Child Adolesc Psychiatry Ment Health*. 2008;2:4.
79. Geurts HM, Corbett B, Solomon M. The paradox of cognitive flexibility in autism. *Trends Cogn Sci*. 2009;13:74-82.
80. Yerys BE, Wallace GL, Sokoloff JL, Shook DA, James JD, Kenworthy L. Attention deficit/hyperactivity disorder symptoms moderate cognition and behavior in children with autism spectrum disorders. *Autism Res*. 2009;2:322-333.
81. Ozonoff S, Cook I, Coon H, et al. Performance on Cambridge Neuropsychological Test Automated Battery subtests sensitive to frontal lobe function in people with autistic disorder: evidence from the Collaborative Programs of Excellence in Autism network. *J Autism Dev Disord*. 2004;34:139-150.
82. Landa RJ, Goldberg MC. Language, social, and executive functions in high functioning autism: a continuum of performance. *J Autism Dev Disord*. 2005;35:557-573.
83. McFarlane HG, Kusek GK, Yang M, Phoenix JL, Bolivar VJ, Crawley JN. Autism-like behavioral phenotypes in BTBR T+tf/J mice. *Genes Brain Behav*. 2008;7:152-163.
84. Bekkers JM, Suzuki N. Neurons and circuits for odor processing in the piriform cortex. *Trends Neurosci*. 2013;36:429-438.
85. Stettler DD, Axel R. Representations of odor in the piriform cortex. *Neuron*. 2009;63:854-864.
86. Savic I, Gulyas B, Larsson M, Roland P. Olfactory functions are mediated by parallel and hierarchical processing. *Neuron*. 2000;26:735-745.
87. Hsieh CP, Chang WT, Lee YC, Huang AM. Deficits in cerebellar granule cell development and social interactions in CD47 knockout mice. *Dev Neurobiol*. 2015;75:463-484.

## SUPPORTING INFORMATION

Additional Supporting Information may be found online in the supporting information tab for this article.

**How to cite this article:** Tantra M, Guo L, Kim J, et al. Conditional deletion of Cadherin 13 perturbs Golgi cells and disrupts social and cognitive behaviors. *Genes, Brain and Behavior*. 2018;17:e12466. <https://doi.org/10.1111/gbb.12466>